Design of a lab-on-a-chip for clinical tests of human physiological fluids

J. M. Miranda*[a], G. Minas[b], A. A. Vicente[a], J. A. Teixeira[a]

[a] Centro de Engenharia Biológica, Universidade do Minho, Campus de Gualtar 4710-057 Braga, Portugal

[b] Department of Industrial Electronics, University of Minho, Campus de Azurém, 4800-058 Guimarães, Portugal

Abstract

Labs-on-a-chip are useful to perform in situ clinical tests with instantaneous results. In this work, the design phase of the development of a lab-on-a-chip is presented. The device will be used to perform tests on physiological fluids. It will be able to test 8 components: calcium, chloride, creatinine, glucose, magnesium, total protein, urea and uric acid. A sample of the physiological fluid reacts with several reagents and the device measures the absorbance of the reaction products.

The lab-on-a-chip is composed of a microfluidic system and an optical detection system. The first contains microchannels and micro-reactors fabricated using SU-8 techniques. The second includes CMOS photodetectors and readout electronics, as well as optical filters fabricated using CMOS-compatible post-processing on top of the photodetectors.

Careful design of the microfluidic system of a lab-on-a-chip requires knowledge of the transport phenomena in the microchannels. Numerical methods are used to simulate the electroosmotic flow, reaction and mixture in the system. Velocity-pressure formulation of the Navier-Stokes equations is solved by a finite difference method. Mass transport equation is solved by a second order finite difference method. For enzymatic reactions, biochemical reaction kinetics is considered.

Design choices are presented and explained. The final design of the microfluidic system complies with layout restriction and kinetic, mass transport and other physical limitations. The dimensions of the micro-reactors are optimized to maximize mixing.

The design of the optical detection system involves selection of the dielectric layers available in the CMOS process for the photodetectors and selection of the dielectric thin-films layers for the optical filters. An array of 8 selective optical filters is designed for parallel testing of the 8 reported components. They are structurally optimized for an optical response at the absorption peak of each reaction product. The lab-on-a-chip output provides a digital signal for computer interfacing.

*Corresponding author. E-mail:jmiranda@gmail.com

1. Introduction

The healthcare sector is nowadays one of the most dynamic and where the novelty is a strategic and operational imperative. The possibility of increasing the quantity and quality of clinical analyses, performed with instantaneous results and outside the clinical laboratories, contributes to a better quality in the health care services and also a better efficiency in the clinical and administrative processes [1].

In recent years, labs-on-a-chip to analyze biological fluids have been developed. They allow the selective measurement of the concentration of biomolecules in biological fluids, with instantaneous results, at any location, with small quantities of reagents and samples and with low-cost.

Labs-on-a-chip are composed of a microfluidic system, in which mixing and reaction takes place, and a sensor system, in which detection and quantification takes place. The microfluidic system is composed of a dispensing zone, a fluid transportation zone and a detection zone. In the dispensing zone the sample and the reactants are supplied to the system. In the transport zone reactants and the sample are mixed and transported to the detection zone. In the detection zone the reaction takes place while followed by some detection mechanism.

Several systems have been developed to perform biochemical reactions[2], including systems with immobilized enzymes[3], medical tests [4], forensic tests[5] and multi-enzyme catalysis[6]. Enzymes may be supplied to the system dissolved into a feed stream [7], enclosed in a separated phase [4] or may be immobilized in the microchannels [3][6]. Immobilization of enzymes require the pretreatment of the surface of the microchannels which may be difficult and unstable and encapsulation in a separated phase requires a mechanism to produce drops or bubbles and so the supply of the enzyme dissolved in the feed stream may be the best alternative for many practical applications.

The problem of fluid transportation in microchannels is of particular importance. Pressure driven flows have some disadvantages that make them unsuitable for some application. Pressure driven flows require external equipment and/or internal moving parts like micro-pumps and micro-valves that require complex manufacturing techniques. Additionally, since the velocity profile in a microchannel is parabolic, pressure driven flows promote

dispersion that may be undesirable.

The electroosmotic flows are an important alternative to pressure driven flows since no external devices or internal moving parts are necessary. Electroosmotic flows result from the electroosmotic phenomenon. When the liquid is an electrolyte, a surface charged negatively (the most common case) becomes covered by a layer of positively charged particles. An electric double layer (EDL) is formed. When an electric field is applied along the surface, the positively charged particles move along the electric field and as they move they drag the remaining of the fluid with them. Since the flow is promoted by the electric field created between electrodes, it can be easily controlled. Moreover, in a microchannel, the velocity profile is uniform and axial dispersion is negligible.

A portable device that ensures analysis within consultation time, at a patient house (allowing a first trial), must have a simple detection mechanism that is independent of any external equipment. Usually, detection relies on fluorescence [7][9][10] and electrochemical detectors [11][12], but a portable device relying on colorimetric detection by the optical absorption in a part of the visible spectrum, compatible with the standard laboratory tests, would be an important alternative to those methods.

In this work, the design phase of the development of a lab-on-a-chip device relying on electroosmotic flow for fluid transport and colorimetric detection methods is presented. The device will be used to perform tests on physiological fluids. It will be able to test 8 components: calcium, chloride, creatinine, glucose, magnesium, total protein, urea and uric acid.

The design of the microfluidic system will be based on Computational Fluid Dynamics techniques. Mixing and reaction of the components of the process must be simulated by solving the flow and mass transport equation. A good design must guarantee the mixing of the reactants to assure a uniform mixture at the detection zone.

2. Description of the device

The lab-on-a-chip studied comprises a microfluidic system (Figure 1) and of a detection system (Figure 2). There are 8 inlets for the reactants and a unique inlet for the sample to

be tested. The sample is mixed with the respective reactants (including the enzymes that catalyze the biological reactions). Initially, the mixing channels are filled with a buffer solution. Then, the sample and the reactant are supplied to the system getting in contact at a T junctions. Mixing and reaction take place along the transportation channel and in the detection zone.

The microchannel for fluid transportation and the detection chamber are 50 μm wide and 500 μm deep. The high depth is crucial for the optical absorption measurements. For each main channel, e.g., for each biomolecule analysis, two additional detection chambers are needed. One, to obtain the baseline reference and to calibrate the light source. The other, to calibrate the biomolecule concentration (with a well-known concentration standard) and also to compensate the white light oscillations.

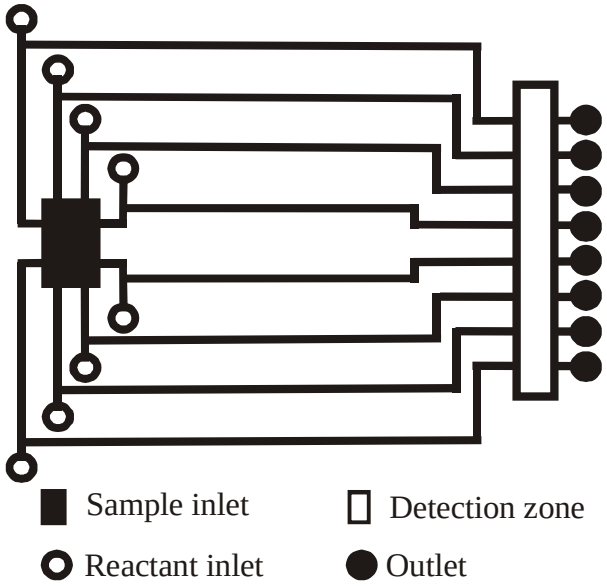

Figure 1 - Scheme of the microfluidic system of the lab-on-a-chip.

The microfluidic system will be fabricated in SU-8 photoresist, which gives the required rectangular vertical profile of the microchannels. The microfluidic system is limited to bi-dimensional layout structures due to the SU-8 based fabrication, i.e., the microchannels can not have different depths for improving the mixing process. Despite this limitation its fabrication is a low-cost process, UV lithography semiconductor compatible and does not require expensive masks. In addition, the microfluidic system can be a disposable die,

which minimizes the cost associated with cleaning of the microchannels and avoids the contamination between analyses. Moreover, SU-8-based processing enables the fabrication of deep microchannels with very low sidewall roughness and is suitable for optical absorption measurement [13].

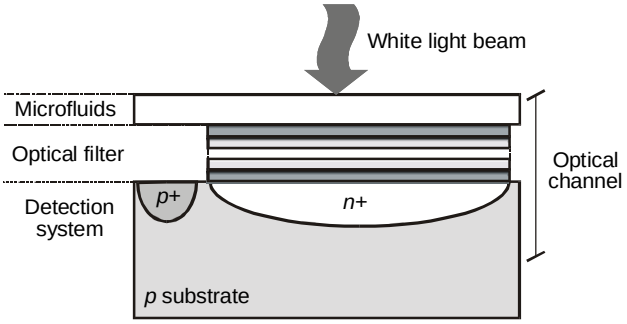

Figure 2. Cross-section of the lab-on-a-chip structure for a single optical-channel.

The optical filters allow the use of only a white light source illumination and should be designed to yield a narrow passband around the wavelength for which the colored mixture being analyzed has its absorption maximum. They allow that the photodiodes measure the intensity of only the desired wavelength transmitted through the mixture. The optical filters are based on highly selective Fabry-Perot thin-films optical resonators fabricated using a stack of dielectric layers (TiO_2 and SiO_2), which offers high reflectivity with low absorption losses [14].

Each optical filter has an active area of $50 \times 50\ \mu m^2$ and is sensitive in a single wavelength with a peak intensity higher than 86% and a FWHM (Full Width Half Maximum) less than 10 nm. They have been designed for analyzing the following biomolecules: calcium, chloride, creatinine, glucose, magnesium, total protein, urea and uric acid, with absorption maximums at 650 nm, 450 nm, 500 nm, 508 nm, 530 nm, 592 nm, 600 nm, 495 nm, respectively.

The photodetectors are placed underneath the detection zone of the microchannels. They convert the light intensity that is transmitted through the colored mixture into a photocurrent. They are designed using the layers available in a CMOS process only, without additional masks or steps [15].

A light-to-frequency converter is integrated with the photodiodes, in the same die, to convert the photocurrent into a digital signal. It produces a bit stream signal with a frequency proportional to the photodiode current and hence proportional to the intensity of the light transmitted through the biological fluid. This digital value is then collect by a microcontroller, which makes the calculations, based on Lambert-Beer's law, to obtain the biomolecule concentration that is being analyzed. The microcontroller also combines data, makes decisions, controls modes and ranges in the photodetectors and provides a standardized output format for higher computer levels.

The CMOS compatible photodetectors and readout circuits have been fabricated through a double-metal, single-polysilicon, 1.6 μm n-well CMOS process. The area of each photodetector is 50×50 μm^2.

3. Theory

3.1. Equations

The electroosmotic flow in the cell is described by Navier-Stokes equations. For a tri-dimensional cell, the dimensionless flow equations are:

$$\nabla \cdot \vec{v} = 0 \tag{1}$$

$$\frac{\partial \vec{v}}{\partial t} + (\vec{v} \cdot \nabla)\vec{v} = -Eu_0 \nabla p + \frac{1}{\mathrm{Re}} \nabla^2 \vec{v} - \prod_1 r_e \nabla \phi \tag{2}$$

where $\vec{v}$ is the velocity vector, t the non-dimensional time (time normalized by τ_W, the residence time based on the channel width), Eu_0 the feed Euler number, Re the Reynolds number, r_e the normalized ionic concentration, p the non-dimensional pressure, ϕ the non-dimensional electric potential and Π_1 a dimensionless number given by:

$$\prod_1 = \frac{FC_0\Phi_0}{M\rho V_0^2} \tag{3}$$

where F is the Faraday constant, C_0 the feed concentration, Φ_0 the potential difference between the entry and the exit of the chip, M the molar mass, ρ is the fluid density and V_0 is the feed velocity.

The Reynolds number is given by:

$$\mathrm{Re} = \frac{\rho V_0 W}{\mu} \tag{4}$$

and the Euler number is given by:

$$Eu_0 = \frac{P_0}{\rho V_0^2} \tag{5}$$

where P_0 is the feed pressure

The Navier-Stokes equations can be written in the velocity-pressure formulation:

$$Eu_0 \Delta p = -\nabla v_x \frac{\partial \vec{v}}{\partial x} - \nabla v_y \frac{\partial \vec{v}}{\partial y} - \Pi_1 \nabla . \left(r_e \nabla \phi \right) \tag{6}$$

$$\frac{\partial \vec{v}}{\partial t} + \left(\vec{v} \cdot \nabla \right) \vec{v} = -Eu_0 \nabla p + \frac{1}{\mathrm{Re}} \nabla^2 \vec{v} - \prod_1 r_e \nabla \phi \tag{7}$$

The pressure-velocity formulation makes possible the split of the computation of the pressure from the computation of the velocity. However, in this formulation it is necessary to introduce a new boundary condition to allow for mass conservation[16] [17] [18]: in addition to the pressure boundary condition, the continuity equation must be satisfied at the wall boundaries.

The normalized ionic concentration is given by:

$$r_e = \sum_{i=1}^{N} z_i c_i \tag{8}$$

where z_i is the electric charge and c_i is the normalized concentration of component *i*. Concentrations are normalized by the concentration of an arbitrarily chosen component, c_1, except for enzyme concentrations which are normalized by their own feed concentration.

The electric potential is related to the ionic concentration by the Gauss equation:

$$\Delta\phi = -\Pi_2 r_e \tag{9}$$

Π_2 is a dimensionless number given by:

$$\Pi_2 = \frac{FC_0H^2}{\varepsilon M \Phi_0} \tag{10}$$

where ε is the permittivity.

The concentration of each ionic species can be determined by solving the mass transport equation (a first order reaction is considered):

$$\frac{\partial c_i}{\partial t} + \vec{v}.\nabla c_i = \frac{1}{Pe}\Delta c_i + \frac{\Pi_3}{Pe}\nabla\left(c_i \nabla\phi\right) - \alpha Dac_1 \tag{11}$$

where c_1 is a reactant, *Pe* is the Peclet number:

$$Pe = \frac{V_0 H}{D} \tag{12}$$

Π_3 is given by:

$$\Pi_3 = \frac{z_i F \Phi_0}{RT} \tag{13}$$

and Da_i is the Damkohler number of reaction *i*:

$$Da_i = \frac{K_i H}{V_0} \tag{14}$$

where K_i is the kinetic constant of reaction *i*.

3.2. Enzymatic reactions

Most of the analytical methods for the analysis of physiological fluids are based on enzymatic reactions. These reactions may be extremely complex involving several intermediate components. To simplify the study, a simple model with 3 components was used. Enzymatic reactions of the form:

$$S \xrightarrow{E} P$$

follow a Michaelis-Menten kinectics. The reaction velocity is given by:

$$-r_S = \frac{K_1 C_E C_S}{K_E + C_S} \tag{15}$$

When the concentration of substrate is low the reaction velocity is given by:

$$-r_S = K C_E C_S \tag{16}$$

The mass transport equation for the substrate, the enzyme and the product are given, respectively, by:

$$\frac{\partial c_S}{\partial t} + \vec{v}.\nabla c_S = \frac{1}{Pe_S}\Delta c_S - Dac_E c_S \tag{17}$$

$$\frac{\partial c_E}{\partial t} + \vec{v}.\nabla c_E = \frac{1}{Pe_E}\Delta c_E \tag{18}$$

$$\frac{\partial c_P}{\partial t} + \vec{v}.\nabla c_P = \frac{1}{Pe_P}\Delta c_P + Dac_E c_S \tag{19}$$

where

$$Da = \frac{KC_E W}{V_0} \tag{20}$$

3.3. Simplified model for long channels

The complete simulation of the flow and mass transport in a long microchannel requires very large meshes. Computational resources may be very high and more sophisticated methods to deal with large domains are required. A complementary approach based on some simplifying assumptions was followed.

In a simple mixer, like the T junction represented in Figure 5, the reactant and the sample follow parallel streams along the mixing channel (Figure 3), and since for electroosmotic flow the velocity in the channel is uniform, the two streams mix exclusively by diffusion in the transversal direction. The mass transport equation in a system of coordinates that moves at the fluid velocity is:

$$\frac{\partial c_i}{\partial t_r} = \frac{1}{Pe}\frac{\partial^2 c}{\partial y^2} - \alpha Dac_1 \tag{21}$$

where t_r is the residence time of the fluid located in (x,y). In the absence of diffusional

limitations, equation (21) becomes:

$$\frac{\partial c_i}{\partial t_r} = -\alpha Da c_1 \tag{22}$$

This equation has an analytical solution and can be used to determine the concentration of the product of the enzymatic reaction described on section 3.2:

$$c_P = 1 - \exp(-Da\, t_r) \tag{23}$$

The initial conditions for t_r=0 are:

$$\begin{cases} c_S(0,y) = 1 \Leftarrow y < 0.5 \\ c_S(0,y) = 0 \Leftarrow y > 0.5 \end{cases} \tag{24}$$

$$\begin{cases} c_E(0,y) = 0 \Leftarrow y < 0.5 \\ c_E(0,y) = 1 \Leftarrow y > 0.5 \end{cases} \tag{25}$$

$$c_P(0,y) = 0 \tag{26}$$

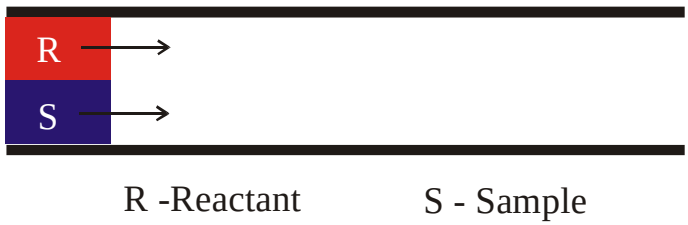

Figure 3 - In a uniaxial flow mixing between two parallel streams results exclusively from transversal diffusion.

3.4. Numerical Method

Some simplifications were made to solve the flow and mass transport equations. The fluid was considered to be a neutral solution with two ionic species. In the electric double layer, since ionic species are in equilibrium, the Boltzmann equation applies:

$$c_i = \exp\left[-z_i \Pi_3 \left(\phi - \phi_b\right)\right] \tag{27}$$

The normalized ionic concentration becomes:

$$r_e = \exp\left[-\Pi_3 \left(\phi - \phi_b\right)\right] - \exp\left[\Pi_3 \left(\phi - \phi_b\right)\right] \tag{28}$$

and equation (9) becomes independent of the flow equations:

$$\Delta\phi = 2\Pi_2 \sinh\left(\Pi_3 \phi_i\right) \tag{29}$$

and can be solved independently.

After the determination of the potential, the Navier-Stokes equations can be solved. These equations were solved by a method similar to the one developed by Henshaw and Petersson [17]. The velocity equations were solved by a second order Bashford-Adams predictor-corrector technique. The viscous terms were treated implicitly and the pressure, the electric force and the convection terms were treated explicitly. Since the convective terms were approximated by a second order central difference method, it was necessary to introduce artificial viscosity for stability. The mass transport equation was solved by a second order finite difference method.

3.5. Numerical limitations

Numerical simulations of the electroosmotic flow are limited by the small thickness of the electric double layer. The small thickness of the EDL means that the mesh required to resolve it must have a very high density near the wall. And, since the time step is proportional to the distance between grid nodes, the time required to solve the problem is very high.

3.6. Test of the code

The code developed was compared with an analytical solutions to test the accuracy of the numerical method. The velocity profile of the electroosmotic flow in a channel was calculated by the code and the results were compared with the analytical solution obtained by Dutta and Beskok [19]. As Figure 4 shows, the numerical method predicts accurately the analytical solution.

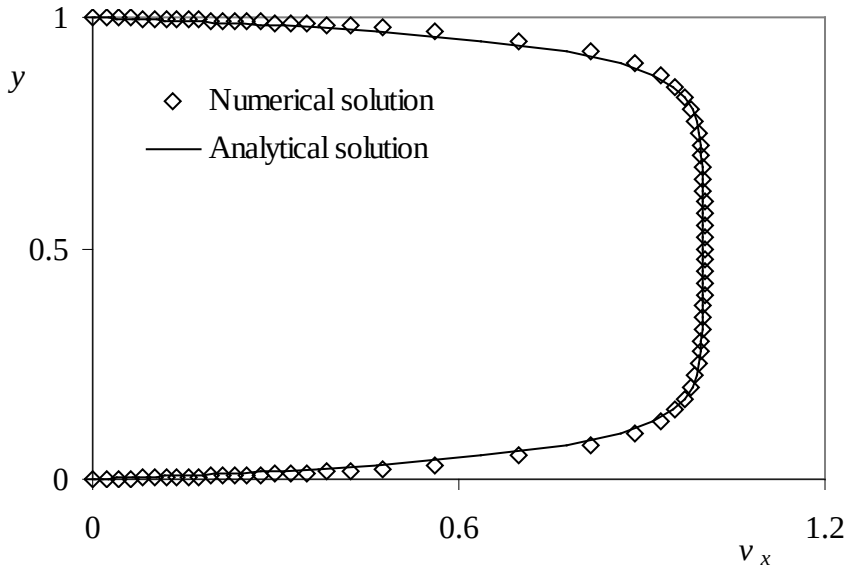

Figure 4 - Velocity profile in the channel (Re=0.96, $\Pi_1=2.14\times10^2$, $\Pi_2=0.01$, $\Pi_3=1.94\times10^4$). Comparison between a numerical solution and the analytical solution from Dutta and Beskok [19].

4. Results and discussion

Detection methods used in this work are standard methods that were adapted to microfluidic systems. The kinetic constant of glucose assay (Trindler method) was determined experimentally in our laboratory and diffusion coefficients were taken from literature. The physiological fluid and solutions containing the reactants are diluted aqueous solutions with the same properties (density, viscosity and permittivity) of water.

The code developed was used to study flow and mass transport in the microfluidic system. The results can be extrapolated to the detection of glucose or other molecules that can be analyzed by enzymatic methods. Simulations were made for $Re = 20$, $Pe_S = 72$, $Pe_P = 100$ and $Pe_E = 1000$. These values were calculated based on the values of table II, except for Pe_P which is a typical value for a small molecule. The geometry considered is a T junction (Figure 5).

The electroosmotic flow in the T junction was determined for an electric potential difference of 6 V. The width of the channel ($W = 50$ μm) was chosen taking in consideration the possibilities of the SU-8 technique. Since the ratio between the depth and the width of the channel is 10:1, the flow was considered to be bi-dimensional. The zeta potential of the SU-8 was taken from Sikanen et. al. [20]. The reference velocity is the velocity in a channel determined by the Shelmholtz-Smoluchowski equation for an electric field of 1 V per each 50 μm.

The applied electric potential creates the fields represented in Figure 6. Figure 6a is the external electric potential generated by the external electrodes and Figure 6b is the internal electric potential generated by the charges in solution. Charge distribution is represented in Figure 7.

Table 1 – Data used to simulate the elecro-osmotic flow

Viscosity	μ	0.001 Kg m^{-1} s^{-1}
Density	ρ	10^3 Kg m^{-3}
Channel width	W	5×10^{-5} m
Permittivity	ε	5×10^{-10} m
Ionic density	ρ_e	3.7×10^{-6} mol m^{-3}
Temperature	T	293 K
Zeta potential	ζ	-0.07 V
Reference velocity	V_0	9.94×10^{-4} m/s
Reference potential	Φ_0	6 V
EDL thickness	λ	5 μm
Residence time (based on the channel width)	τ_W	5.03×10^{-2} s

Table 2 – Mass transport data

Glucose diffusion coefficient	$D_{glucose}$	6.9×10^{-10} m^2s^{-1}
Glucose oxidase diffusion coefficient	$D_{glucosidase}$	4.94×10^{-11} m^2s^{-1}
Kinetic constant	K	0.00623 s^{-1}

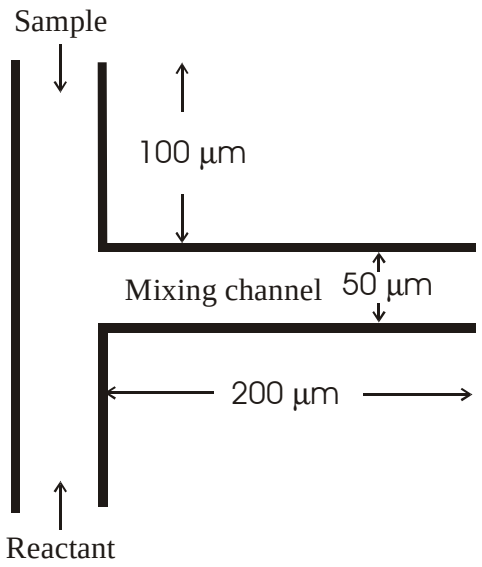

Figure 5 – T junction.

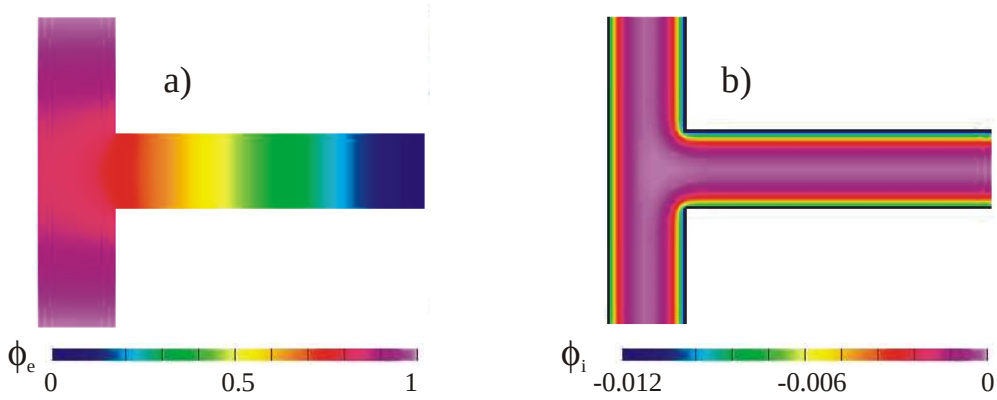

Figure 6 – Electric potential (Π_1=2.18×10^3, Π_2=0.211, Π_3=237). a) External electric potential; b) Internal electric potential.

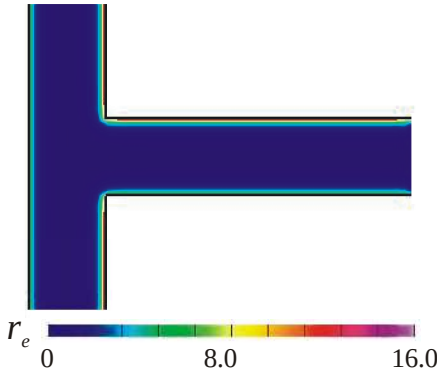

Figure 7 – Charge distribution (Π_1=2.18×10^3, Π_2=0.211, Π_3=237).

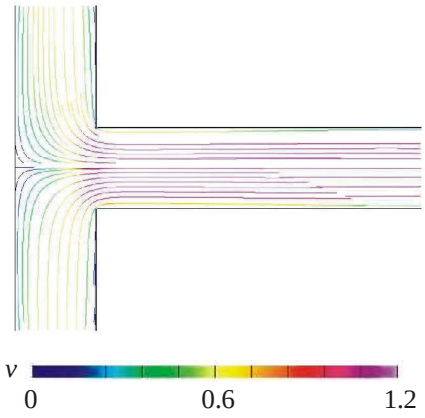

Figure 8 – a) Electroosmotic flow (Π_1=2.18×10^3, Π_2=0.211, Π_3=237, Re=0.05).

For a uniaxial flow, the channel length required for mixing is roughly equal to $Pe \times W$ [21]. This mixing length can be prohibitively long if the flow velocity is too high and the diffusion coefficient of at least one of the components is too small. In enzymatic reactions, the diffusion coefficient of the enzyme is usually the limiting factor.

Figure 9 shows the results for mass transport and reaction in the T junction. Reaction takes place along the axis of the transport channel. Since the enzyme diffuses slowly to the sample stream, and the substrate diffuses faster to the reactant stream, the reaction takes place mainly in the enzyme side of the microchannel.

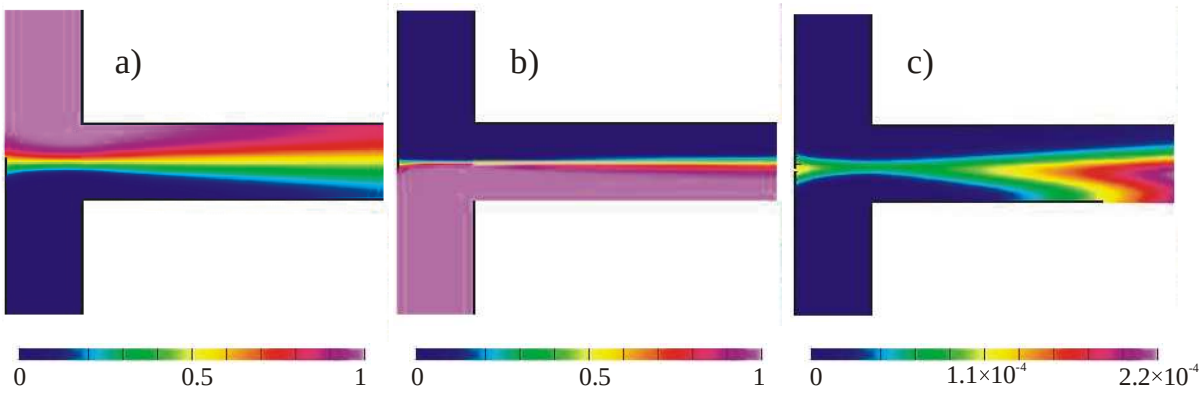

Figure 9 – Mass transport and reaction in the T junction for Re=0.05, $\Pi_1=2.18\times10^3$, $\Pi_2=0.211$, $\Pi_3=237$, $Pe_S=72$, $Pe_E=1000$ and $Pe_P=100$. a) Substrate concentration; b) Enzyme concentration; c) Product concentration.

The results of Figure 9 are for mass transport in a short mixing channel (the length of the channel is only 4*W*). For longer channels, the simplified approach described on section 3.3 was followed. Two quantities were determined: the mixing time as a function of the Peclet number in the absence of reaction and the concentration of the product of a typical enzymatic reaction as a function of the residence time.

Numerical results obtained for several Peclet numbers (Figure 10) show that mixing times increase significantly with Peclet. When *Pe*=1000, the non-dimensional mixing time is 500 τ_W, which means that for a 50 μm channel the residence time necessary for complete mixing is 25 s.

Note that the mixing process occurs while the fluid is transported to the detection zone and

may continue after the fluid gets there. At the same time, the enzyme will promote reaction during all the mixing process so that when the fluid is well mixed the concentration of the substrate is no longer at its initial concentration. Figure 11 is the representation of the concentration of P as a function of the non-dimensional time for $Pe_S = 72$, $Pe_P = 100$ and $Pe_E = 1000$. The symbols are the numerical results and the line is an analytical result obtained for no diffusional limitations — equation (23). For the time scale considered, diffusional limitations do not interfere with the reaction rate. This happens because, although the mixing time of the enzyme is 500 τ_w, the mixing times of the substrate and the product are much smaller (less than 50 τ_w). For a significantly amount of time, the reaction takes place in the enzyme side of the channel in a smaller volume but at a higher rate.

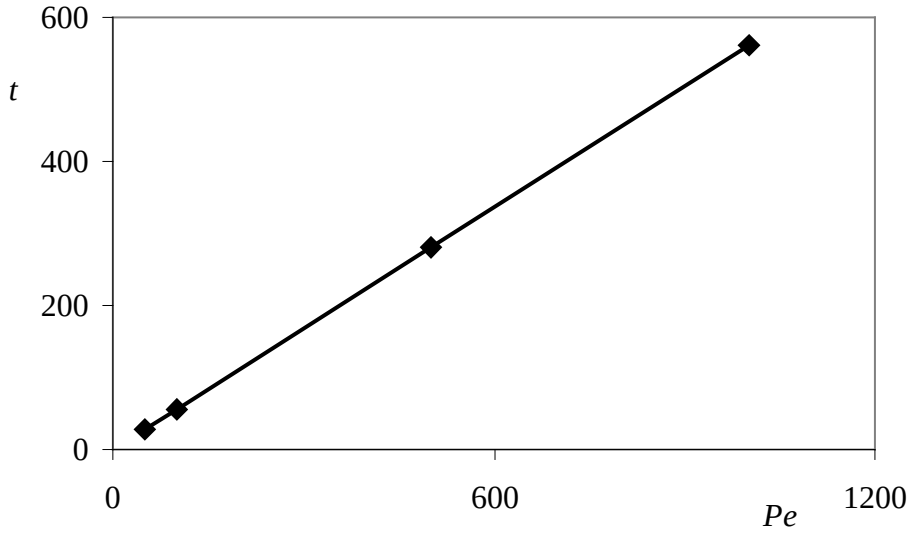

Figure 10 – Non-dimensional mixing time as a function of the Peclet number.

The results obtained impose some restrictions to the mode of operation of the lab-on-a-chip. Two possible modes of operation can be adopted. In continuous flow, the concentration in the sample is determined from the concentration of the product in the detection zone when the flow and mass transport get to the steady state. The length of the channel must be such that the residence time in the channel is higher than the mixing times of the substrate and the product. The mixing time of the substrate must be negligible. This mode of operation has the disadvantage that the concentration of the substrate is determined from a unique measurement of the concentration of the product. Alternatively, a semi-continuous mode of

operation can be used. In this mode of operation, the system works in continuous flow until it reaches the steady state. Then, the flow is shut-down. When the flow is shut-down the detection chamber works as a closed reactor. The reaction can then be followed by the measuring device and the data collected can be used to determine the substrate concentration by the method of the initial velocities.

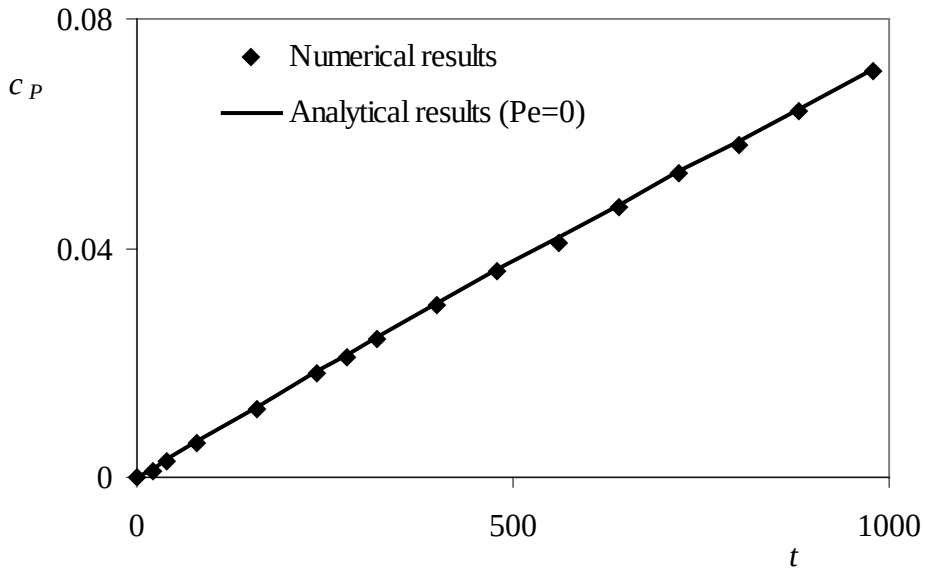

Figure 11 – Concentration of the product P as a function of non-dimensional time (Pe_S=72, Pe_E=1000, Pe_P=100, $Da=3.13\times10^{-4}$). The analytical results were determined by equation (23).

5. Conclusion

The design of a lab-on-a-chip for clinical tests of human physiological fluids was reported. The appropriate study of the mixing and the reaction of a sample with the reactants in the microfluidic system has involved the use of numerical methods to solve the flow and mass transport equations. For enzymatic reactions, the mixing is limited by the diffusion coefficient of the largest molecule, usually a enzyme. The flow and mass transport in a T junction were studied and mixing times were determined for the case of glucose analysis. The same analysis can be applied to the remaining molecules.

Acknowledgments

Support for this research was provided by the R&D Centre Algoritmi, the Engineering School of University of Minho (program IN^{2}TEC) and the Portuguese Science Foundation (grant SFRH/BPD/17689/2004 awarded to J. M: Miranda)

Nomenclature

C_0	Reference concentration
c	Non-dimensional concentration
c_S	Non-dimensional substrate concentration
c_E	Non-dimensional enzyme concentration
c_P	Non-dimensional product concentration
D	Diffusion coefficient
F	Faraday constant
L	Length of the channel
M	Molecular mass
N	Number of ionic species in solution
P_0	Reference pressure
p	Non-dimensional pressure
r_e	Non-dimensional ionic density
T	Temperature
t	Non-dimensional time
t_m	Mixing time
t_r	Residence time based on the distance travelled by the fluid
t_{react}	Reaction time
V_0	Feed velocity
$\vec{v}$	Non-dimensional velocity vector
v_y	Non-dimensional longitudinal component of the velocity
v_x	Non-dimensional axial component of the velocity
W	Channel width
z	Electric charge

Greek symbols

ε	Permittivity
Φ	Electric potential
Φ_0	Electric potential between the sample inlet and the detection chamber
ϕ	Non-dimensional electric potential
ϕ_i	Non-dimensional internal electric potential
ϕ_e	Non-dimensional external electric potential
ϕ_b	Non-dimensional electric potential in the bulk
μ	Fluid viscosity
ρ	Fluid density
ρ_e	Ionic density
τ_W	Residence time based on the width of the channel
ζ	Zeta potential

Non-dimensional numbers

Da	Damkohler
Eu_0	Euler number
Pe	Peclet number
Π_1	$\frac{FC_0\Phi_0}{M\rho V_0^2}$
Π_2	$\frac{FC_0H^2}{\varepsilon M\Phi_0}$
Π_3	$\frac{z_iF\Phi_0}{RT}$
Re	Reynolds number

Bibliography

[1] P. Connolly, Clinical diagnostics opportunities for biosensors and bioelectronics Biosensors & Bioelectronics, 10, 1-6, (1995).

[2] U. Bilitewski, M. Genrich, S. Kadow, G. Mersal, Biochemical analysis with microfluidic systems, Anal Bioanal Chem, 377, 556−569, (2003).

[3] H. Mao, T. Yang, and P. S. Cremer, Design and Characterization of Immobilized Enzymes in Microfluidic Systems, Anal. Chem., 74, 379-385 (2002).

[4] V. Srinivasan, V. K. Pamula and R. B. Fair, An integrated digital microfluidic lab-on-a-chip for clinical diagnostics on human physiological fluids, Lab on a Chip, 4, 310-315, (2004).

[5] E. Verpoorte, Microfluidic chips for clinical and forensic analysis, Electrophoresis, 23, 677–712, (2002).

[6] M.-Y. Lee, A. Srinivasan, B. Ku, J. S. Dordick, Multienzyme Catalysis in Microfluidic Biochips, Biotecnnology and Bioengineering, 83, (2003).

[7] N. F. de Rooij, and R. Dändliker, Fabrication of Multilayer Systems Combining Microfluidic and Microoptical Elements for Fluorescence Detection, Journal of Microelectromechanical Systems, 10, (2001).

[8] A. G. Hadd, D. E. Raymond, J. W. Halliwell, S. C. Jacobson, and J. M. Ramsey, Microchip Device for Performing Enzyme Assays, Anal. Chem., 69, 3407-3412, (1997).

[9] J. C. Roulet, R. Volkel, H. P. Herzig, E. Verpoorte, N. F. de Rooij, and R. Dandliker Performance of an Integrated Microoptical System for Fluorescence Detection in Microfluidic Systems, Anal. Chem., 74, 3400-3407, (2002)

[10] M. L. Chabinyc, D. T. Chiu, J. C. McDonald, A. D. Stroock, J. F. Christian, A. M. Karger, and G. M. Whitesides, An Integrated Fluorescence Detection System in poly(dimethylsiloxane) for Microfluidic Applications, Anal. Chem., 73, 4491-4498, (2001).

[11] N. A. Lacher, K. E. G., R. S. Martin, S. M. Lunte, Microchip, capillary electrophoresis/ electrochemistry, Electrophoresis, 22, 2526 – 2536**, (**2001).

[12] W. R. Vandaveer IV, S. A. Pasas, R. S. Martin, S. M. Lunte, Recent developments in amperometric detection for microchip capillary electrophoresis, Electrophoresis, 23, 3667–3677, (2002).

[13] SU-8: A Thin Photo-Resister for MEM's, http://aveclafaux.freeservers.com/SU-8.html

[14] G. Minas, R. F. Wolffenbuttel, J. H. Correia, A Lab-on-a-Chip for Spectrophotometric Analysis of Biological Fluids. In Lab-on-a-Chip, The Royal Society of Chemistry, 5, , 1303-1309, (2005).

[15] G. Minas, J.S. Martins, J.C. Ribeiro, R.F. Wolffenbuttel and J.H. Correia, Sensors and Actuators, A110, 33-38, (2004).

[16] N. A. Petersson, Stability of Pressure Boundary Conditions for Stokes and Navier–Stokes Equations, Journal of Computational Physics, 172, 40–70 (2001)

[17] *W. D. Henshaw, N. A. Petersson,* A Split-Step Scheme for the Incompressible Navier-Stokes Equations, Workshop on Numerical Simulations of Incompressible Flows Half Moon Bay, CA, June 19-21, (2001).

[18] W. D. Henshaw, A fourth-order accurate method for the incompressible Navier-Stokes equations on overlapping grids, Journal of Computational Physics, 113 , 1, 13 - 25 (1994).

[19] P. Dutta and A. Beskok, Analytical Solution of Combined Electroosmotic/Pressure Driven Flows in Two-Dimensional Straight Channels: Finite Debye Layer Effects, Anal. Chem., 73, 1979-1986 (2001).

[20] T. Sikanen, S. Tuomikoski, R. A. Ketola, R. Kostiainen, S. Franssilab and T. Kotiaho, Characterization of SU-8 for electrokinetic microfluidic applications, Lab Chip, 5, 888-896, (2005).

[21] A. D. Stroock, S. K. W. Dertinger, A. Ajdari, I. Mezic, H. A. Stone, G. M. Whitesides, Chaotic Mixer for Microchannels, Science, 295, (2002).